ARTICLE

Drying Enhanced Adhesion of Polythiophene Nanotubule Arrays on Smooth Surfaces

Gewu Lu,[†] Wenjing Hong,[†] Lei Tong,[†] Hua Bai,[†] Yen Wei,[‡] and Gaoquan Shi[†,*]

[†]Department of Chemistry and Laboratory of Bio-organic Phosphorus, Tsinghua University, Beijing 100084, People's Republic of China, and [‡]Department of Chemistry, Drexel University, Philadelphia, Pennsylvania 19104

ABSTRACT Polythiophene (Pth) films with aligned nanotubule arrays were adhered strongly on various smooth surfaces such as glass, mica, and GaAs after drying from their wet states under ambient condition. The normal and shear dry adhesion forces of the films on glass with contact areas of 0.5−1.0 cm^2 were measured to be 80 ± 8 and 174 ± 10 N cm^{-2}, respectively. These extraordinary strong adhesion forces are attributed to the high strength and stiffness of Pth and the high contact fraction (~79%) of Pth nanotips on the smooth surfaces induced by drying. During the drying process, there is little controlled preload, suggesting a real gecko-like adhesion of Pth nanotubule arrays.

KEYWORDS: adhesion · friction · polythiophene · drying · nanotubule

Inspired by the micro- and nanobinary structures and the composition of gecko foot, various micro- and nanostructured polymer films and carbon nanotube arrays have been explored for dry adhesives.[1−15] The adhesion forces of the adhesives with nanohair arrays are mainly attributed to the interfacial interactions of synthetic nanohairs with target surfaces and are usually limited by the low contact fractions of the nanohairs.[16,17] To fabricate strong adhesives, the nanohairs are suggested to be synthesized from materials with high mechanical properties.[18] Furthermore, the nanohairs should have high aspect ratios to provide sufficient flexibility, and their stiffness and number density also have to be maximized.[18] In this paper, we report nanohair adhesives based on bilayered polythiophene (Pth) films that have an aligned Pth nanotubule layer and a compact Pth layer. The electrochemically synthesized Pth was chosen as the starting material because of its high Young's modulus (1.5 GPa) and tensile strength (120−130 MPa) and great flexibility.[19] The Pth bilayer films adhered strongly with their aligned nanotubule arrays on various smooth surfaces such as glass, mica, GaAs, and plastics after drying from their wet states under ambient condition. The normal (adhesion) and shear (friction) forces of the films with contact areas of 0.5−1.0 cm^2 on glass were found to be 80 ± 8 and 174 ± 10 N cm^{-2}, respectively; the macroscopic achievable shear force is about 18 times that of a gecko foot. It was found that the drying process induced a high contact fraction of Pth nanotips on target surfaces and greatly enhanced the adhesion and friction forces.

RESULTS AND DISCUSSION

The Pth bilayer films were synthesized by electrochemical polymerization of thiophene in boron trifluoride diethyl etherate (BFEE) using porous anodic aluminum oxide (AAO) membrane as a template (see Methods).[20] The nanotubules have diameters of 200 nm and lengths of 8−20 μm (Figure 1). Therefore, the aspect ratios of the nanotubules are calculated to be about 40−100. The mouths of the nanotubules with a length of 8 or 11 μm are open (Figure 1a,b), while those of the 20 μm tubules are sealed (Figure 1c). The nanotubules are aggregated into bundles because of their high specific surface areas and the capillary forces during drying.[21] However, the nanotubules roughly stand upright on the compact layer without serious lateral collapse and matting (Figure 1d−f). The thickness of the compact layer was controlled to be 2 μm, and the outmost surface of this layer is rough and compact (Figure 1g and inset). The compact layer provides the film with good mechanical strength. It is also thin enough to keep the flexibility of the film. The surfaces of Pth nanotubules were characterized by Raman and X-ray photoelectron energy spectroscopies, which indicate

*Address correspondence to gshi@mail.tsinghua.edu.cn.

Received for review July 15, 2008 and accepted October 28, 2008.

Published online November 8, 2008. 10.1021/nn800443m CCC: $40.75

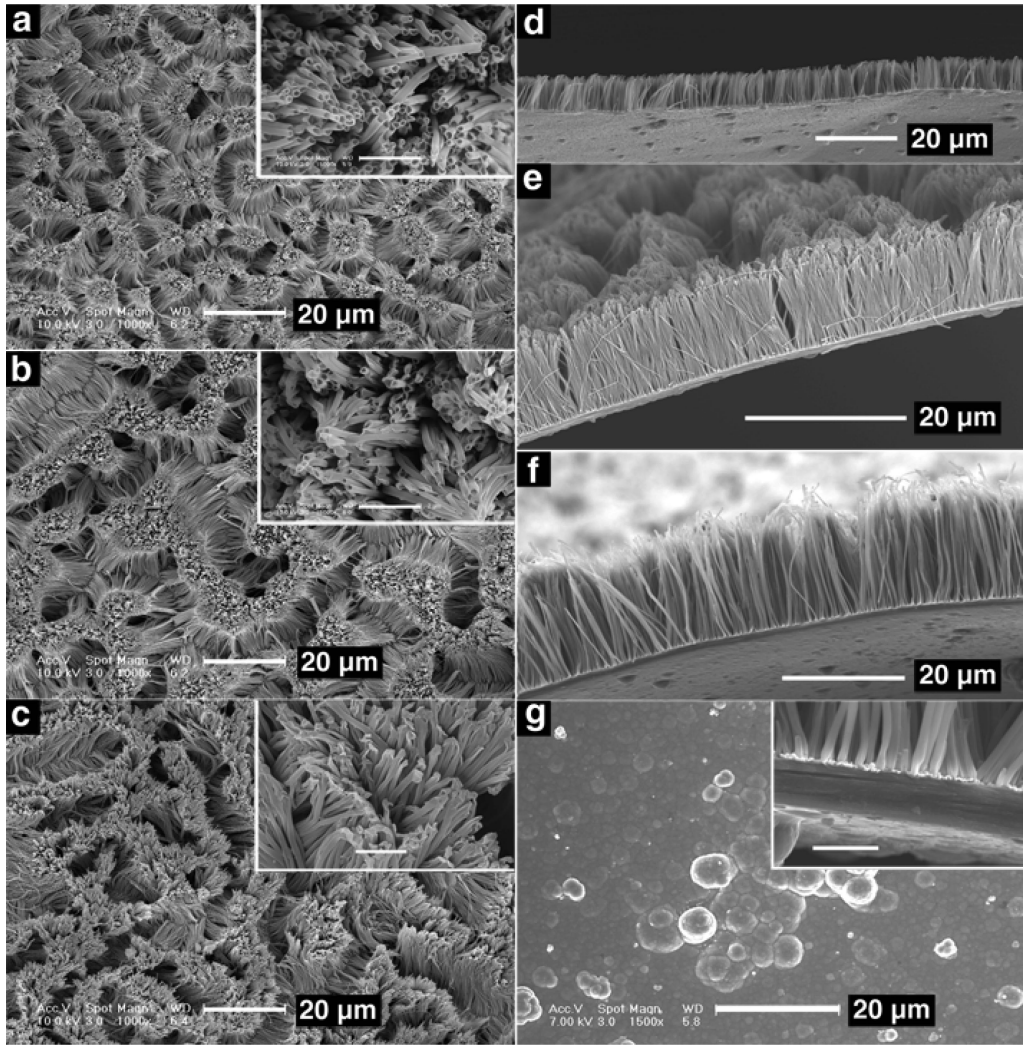

Figure 1. SEM images of the Pth bilayer films. (a−c) Top views of the tubule surfaces with 8 (a), 11 (b), and 20 μm (c) tubules. Insets are the corresponding magnified views. (d−f) Side views of the bilayer films corresponding to a−c. (g) Top view of the compact layer of a bilayer film. Inset is a cross section view. Inset bar scale = 2 μm.

that the tubules are made of polythiophene in the neutral state (Supporting Information, Figure S3).[20] The treatments of the tubules by aqueous solution of KOH during the template removing process and successive washing extensively removed the doping ions and impurities of the polymer.

To investigate the adhesion force, a Pth bilayer film in the wet state was collected by a clean glass sheet with its aligned nanotubule array in contact with the glass surface. The solvent was deionized water or 90% ethanol. The sample on the glass slide was dried in air at ambient temperature for over 1 day (for water) or 5 h (for 90% ethanol) prior to adhesion and friction force measurements (Figure 5 in Methods). The tubule surface of a bilayer film adhered strongly on the smooth surface of a glass sheet after drying from its wet state. The dry adhesion and friction forces of the bilayer films by using both solvents were measured to be essentially the same, and they depend on the length of the tubules. The normal ($F_{\perp}$) and shear ($F_{\parallel}$) forces tested at a slow stretching rate of 0.05 mm min^{-1} (Supporting Information, Figure S4) increase as the tubule length increased from 5 to 11 μm, then they decrease gradually (Figure 2). The longer tubules are more flexible, which is favorable for the attachment of their tips on the target surface and contributes a higher adhesion force. However, entangled segments were observed on the top surface of the 20 μm tubules (Figure 1c), which greatly decreased the overall adhesion force.[14,17] Furthermore, the polydispersity of tubule heights also increased with the increase of tubule length (Figure 1), which also reduced the contact fraction of the nanotips on the target surface and decreased the adhesion forces. The bilayer film with tubule length of ~11 μm and area of 0.5−1.0 cm^2 showed the optimum forces of $F_{\perp} = 80 \pm 8$ N cm^{-2} and $F_{\parallel} = 174 \pm 10$ N cm^{-2}. They are ~8 and ~18 times that of the overall adhesion force of a gecko foot, respectively. Therefore, it is possible to hold a 70 kg person by using the shear adhesion force of only a 4 cm^2 Pth bilayer film.

The excellent adhesion properties of the Pth bilayer film (the length of the Pth tubules was controlled to

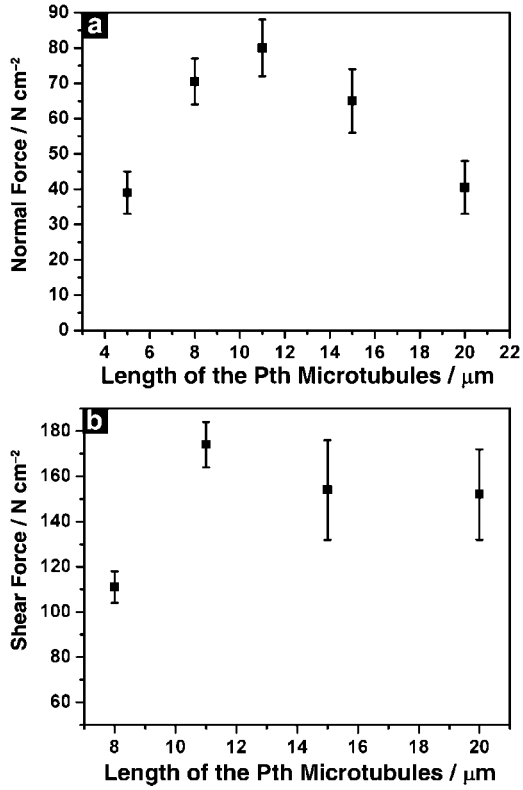

Figure 2. Plots of normal or shear force *versus* Pth tubule length. (a) Normal force. (b) Shear force. For Pth bilayer films with the same tubule length, the normal or shear force was measured for at least 10 repetitions with mean value and standard derivation shown. Film area = 0.5−1.0 cm^2, stretching rate = 0.05 mm min^{-1}.

be 11 μm) on a glass surface in both normal and shear directions were further verified by a homemade cantilever. Figure 3a shows a 0.8 cm^2 bilayer film dry adhered on the surface of a glass sheet being hung by a 6.5 kg weight, corresponding to a normal force of 81 N cm^{-2}. The weight can be stably hung for a long time without detachment (we tested for 35 days). However, as a 7 kg weight (corresponding to a normal force of 88 N cm^{-2}) was hung to the hoop, the bilayer film detached from the glass surface within 2 min. These results confirmed the adhesion forces measured by stretching at slow constant rate described above. After detachment, the film kept its original shape and size, without any dark dots remaining on the glass surface (Figure 3b). The nanotubules of the detached film deformed but still stood well on the Pth dry adhesive tape in bundles (Figure 3c and inset). The tips of tubule bundles adhered together to form a flat surface for perfect interfacial contact.[22,23] The chemical structure and composition of the surface were characterized to be the same as those of the surface of original Pth nanotubule arrays. The dry adhered Pth bilayer film can be detached automatically from the glass surface by immersing the sample into water for over 2 h, mainly due to the absorption of water molecules on the hydrophilic glass surface, which reduces the adhesion.[24] This result also indicates that the dry adhesion of the bilayer film is attributed to the weak intermolecular interactions such as van der Waals force, hydrogen bonding, and capillary effect. The adhesion forces were also found to depend strongly on the polarizability (γ_p, polarity part of surface energy, Supporting Information) of the target surfaces. For examples, on the surfaces of mica (γ_p = 89 mJ m^{-2}), GaAs (γ_p = 27 mJ m^{-2}), poly(methyl methacrylate) (PMMA, γ_p = 17 mJ m^{-2}), and Teflon (γ_p = 4 mJ m^{-2}), the macroscopic achievable normal adhesion forces were tested to be 120, 80, 20, and 2 N cm^{-2}, respectively (Figure 3d). It is interesting to find that the adhesive tape has high adhesion forces on both highly polarizable surfaces, such as glass and mica, and less polarizable surfaces, such as GaAs and PMMA. The adhesion force of the Pth bilayer film on a relatively hydrophobic GaAs surface (80 N cm^{-2}) is close to that on a hydrophilic glass surface (88 N cm^{-2}). These results also indicated that the dry adhesion forces mainly result from van der Waals force, and the contributions of hydrogen bonding and capillary effects are relatively minor.[23] This is possibly due to the fact that Pth lacks functional groups for forming strong hydrogen bonds. The Pth bilayer films, like gecko feet, fail to adhere to the weakly polarizable surface of Teflon because of much reduced van der Waals forces.[23]

Figure 4a shows a 0.5 cm^2 Pth bilayer film dry adhered on a glass surface and being dragged by a 7.5 kg weight in shear direction, corresponding to a shear adhesion force of 150 N cm^{-2}. This system is also stable for a long time (we tested for 35 days) without detachment (Supporting Information, Figure S5). This phenomenon is different from that of a viscoelastic tape (*e.g.*, 3 M Scotch tape) reported by Ge *et al.*[13] The adhesion force of the viscoelastic tape was found to decrease quickly within 100 s during the shear stretching process. Figure 4b shows the typical force of a bilayer film pulled parallel to the surface at a stretching rate of 0.05 mm min^{-1}. The overall features of this figure are similar to those of single gecko seta pulled parallel on a glass surface under a perpendicular preload.[1] This curve can be divided into three stages, corresponding to (I) sample deformation, (II) sliding on the surface to give the maximum shear force, and (III) film pull-off from the surface. More importantly, according to the data described above, the shear adhesion force is about twice that of the normal adhesion force (*i.e.*, $F_{\parallel} = 2.17\ F_{\perp}$). This value is nearly the same as that of gecko seta array ($F_{\parallel} = 2.15\ F_{\perp}$).[22] The phenomenon can be explained by the fact that the Pth nanotubules were bent to a shape similar to a gecko's setae during the pull parallel process (Figure 4c,d). Under shear deformation, the tubules with curvatures along the drag direction were in a compressed state to give an unusually high friction like a gecko seta array.[22] Finally, when the pull parallel force is strong enough, the nanotips of tubules are detached from the target surface and start to slide

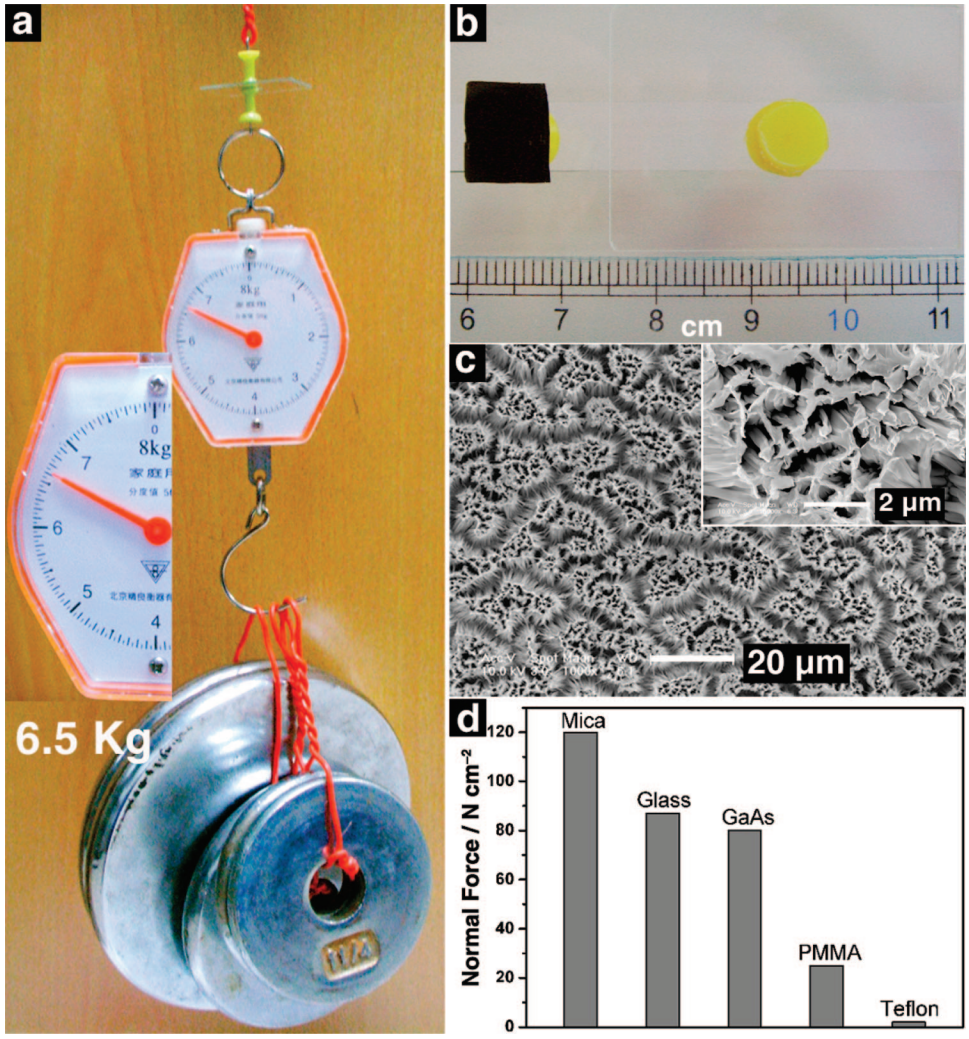

Figure 3. Pth bilayer film pulled in normal direction. (a) Photograph showing a 6.5 kg weight hanging on a glass sheet supported Pth bilayer dry adhesive film; inset indicates the scale of a spring balance. (b) Photograph showing the dry adhesive film detached from the glass (left) and the target glass surface after detachment (right). (c) SEM image of the dry adhesive film after pulling off normally from the glass; inset is a high magnification view. (d) A comparison of the maximum achievable normal force of the bilayer dry adhesive film on mica, glass, GaAs, PMMA, and Telfon. Film contact area = 0.8 cm^2 (0.8 cm × 1.0 cm) and the length of Pth nanotubules = 11 μm.

off. After detachment, the nanotips formed a flat surface (Figure 4e).

The nanotip morphology of the bilayer films cannot be recovered to the original state in air after detaching from the substrates. As a result, the normal adhesion force of a reused film on glass decreased to be only 3 N cm^{-2}. However, when the detached film was treated by cyclic voltammetric scanning or washing with aqueous solutions of detergents or KOH, its adhesive properties can be mostly recovered like many other fibril adhesives (Methods).[15]

The extraordinary high dry adhesion forces of the Pth bilayer films could be attributed to the high aspect ratio (40−100) and high density (1.91×10^9 tubules cm^{-2}, the pore density of the AAO membrane[25]) of the Pth tubules, and to the excellent mechanical properties of Pth films. More importantly, the drying process greatly improved the contact fraction of the Pth nanotips to the target surface. The excellent mechanical properties of Pth resulted in the formation of nonmatting nanotubule arrays as shown in Figure 1, whereas the nanohairs of usual polymers such as polyimide and polyesters with high aspect ratios easily form self-stuck mats.[18] Furthermore, the high modulus and mechanical strength of the Pth nanotubules made them bent rather than lateral and collapse between neighboring nanotubules during the pull parallel process.

Electrosynthesized Pth is a conjugated heteroaromatic polymer with delocalized chain structure. It is insoluble, intractable, and decomposed before melting. Dynamic mechanical test indicated that the real and loss moduli of the Pth film was kept nearly constant in the temperature scale of 25 to 250 °C, and the loss modulus is only 0.05 to that of real modulus.[19] The stress−strain curve of Pth film is linear and does not show a yield point. In addition, the normal adhesion force of a Pth bilayer film on glass is also increased linearly with the displacement of sample. We also mea-

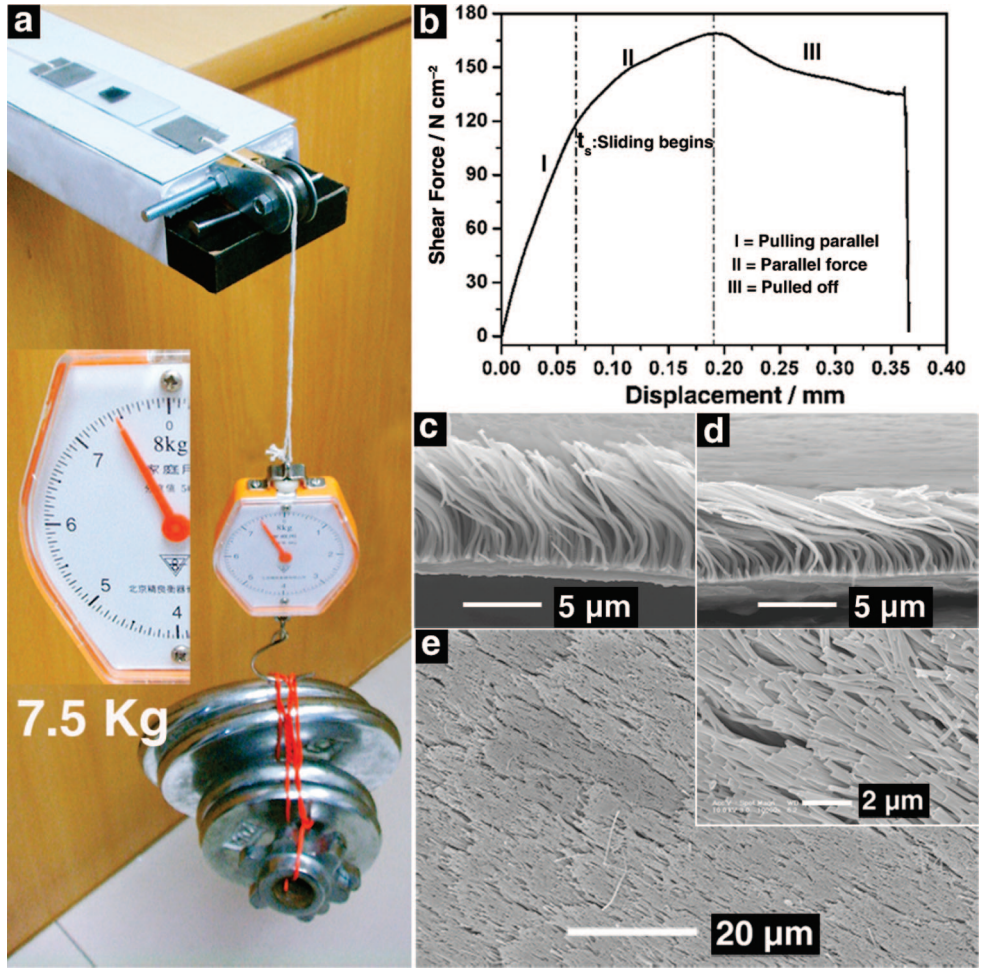

Figure 4. Pth bilayer film pulled in shear direction. (a) Photograph showing a 7.5 kg weight pulling parallel on a glass sheet supported Pth bilayer dry adhesive film; inset showing the scale of a spring balance. (b) Shear adhesion force recorded during pulling parallel on a glass sheet supported Pth bilayer dry adhesive film at a stretching rate of 0.05 mm min^{-1}. (c) Side view SEM images of the dry adhesive film recorded during the pulling parallel process. (d) Side view SEM images of the dry adhesive film recorded after detached from the glass substrate. (e) Top view SEM images of the adhesive after detaching from the glass by pulling parallel; inset is a high magnification view. Film contact area = 0.5 cm^2 (0.7 cm × 0.7 cm) and the length of Pth nanotubules = 11 μm.

sured the normal adhesion force of the Pth bilayer film dry adhered on glass by stopping the stretching before detachment for several seconds and then restretching the same sample. The normal force measured through this two-step process was found to be the same as that by one-step stretching, indicating the nanotubules exhibited elastic deformation under stretching. Therefore, it is reasonable to conclude that the dry Pth bilayer film is an elastic material. Actually, the nanotips of the Pth nanotubule array showed plastic deformation induced by drying (Figure 3c). Pth bilayer film in the wet state was plasticized by water or alcohol; however, after drying, it recovered to its elastic state. The adhesion is attributed to the interaction of elastic dry Pth nanotips with target surface. The normal dry adhesion force between an elastic spherical tip with radius of R and flat surface is given by the Johnson−Kendall−Roberts (JKR) theory as $F = 1.5\pi RW_{12}$, $W_{12} = \gamma_1 + \gamma_2 - \gamma_{12} \approx 2(\gamma_1\gamma_2)^{1/2}$ is the work of adhesion, γ_1 and γ_2 are the surfaces energies of spherical tip and the substrate, respectively, and γ_{12} is the interfacial energy.[18,26] For the Pth films used here, γ_1 measured by Owens−Wend−Rabel−Kaelble (OWRK) method to be 54 mJ m^{-2} and γ_2 for a glass sheet was measured to be 70 mJ m^{-2} (Supporting Information).[27−29] Therefore, 111 N cm^{-2} pull-off force is theoretically expected taking R = 100 nm and the tubule density of 1.91 × 10^9 tubules cm^{-2} for calculation and assuming all the nano-

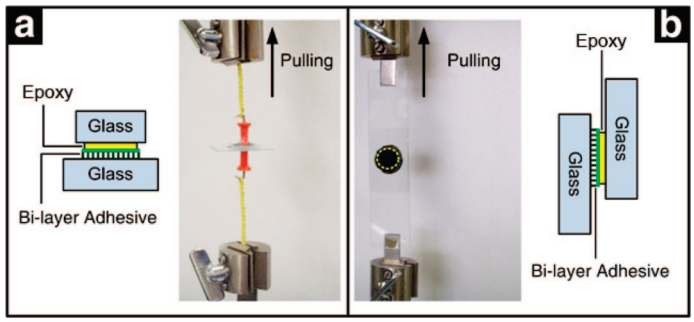

Figure 5. Setup pictures and geometries used for the force measurements. (a) In normal direction. (b) In shear direction.

tips interacted with the target surface.[25] This theoretical value overrated the real case if considering the polydispersity of nanotubule heights. Therefore, the macroscopic achievable 88 N cm^{-2} normal adhesion force (pull-off force) indicated that at least 79% nanotips interacted with the surface. This value (79%) is much higher than that of physically pressed multiwalled carbon nanotube array on glass (<10%).[17] The high contact fraction of the nanotips was induced by drying. During the drying process, the liquid layer between the nanotubule surface and the target surface creates an attractive capillary force that is sufficiently strong to pull the Pth nanotips into contact with the target surface.[30] Hence, the nanotips are adhered to the substrate surface following the drying process. During this process, there is little or no controlled preload, suggesting a real gecko-like adhesion.[31] For calculating the van der Waals contribution to these adhesion forces, $F_{vdW} = HR/6d_0^2$ is used, where $R = 100$ nm is the radius of the nanotubule, $d_0 \approx 165$ nm is the approximate interfacial cutoff distance, and H is the Hamaker constant.[18] Using $H = 60.5 \times 10^{-21}$ for polythiophene (close to that of polyester), 37 nN adhesion force for a single Pth tubule and a total force of 61 N cm^{-2} (for 79% nanotip attachment) were estimated.[18] Therefore, about 69% of the adhesion force of the Pth bilayer film (88 N cm^{-2}) is due to the van der Waals force, while the rest could be due to the secondary adhesion forces and surface roughness effects. As control experiments, a physically pressed Pth bilayer film with the tubule surface in contact with glass substrate showed a weak normal adhesion force of <5 N cm^{-2}. Likewise, a wet flat Pth film without microtubules detaches from the glass surface automatically during the drying process because of a small contact area and the heterogeneity of the flat film in the vertical direction.[32]

CONCLUSIONS

In summary, Pth nanotubule arrays exhibited strong adhesions on various smooth surfaces after drying from their wet states. The macroscopic achievable shear adhesion force of the Pth bilayer film with Pth nanotubule arrays on glass was measured to be about 18 times that of a gecko foot. Drying the wet nanostructured Pth films on both hydrophilic and hydrophobic substrates has induced high contact fractions of the Pth nanotips on the target surfaces and enhanced the adhesion forces greatly. This simple technique can be used in numerous other similar systems. The easy fabrication of the films into large areas with desired shapes and the high adhesion forces of the films make our work as presented here highly promising for practical applications in dry adhesion things with various shapes, sizes, and weights. In addition, electrochemically restorable adhesion based on our materials may lead to gecko-like robotic devices.

METHODS

Fabrication of Pth Bilayer Films. The procedures for preparing the bilayer films are schematically illustrated in Figures S1 and S2 in Supporting Information. Electrochemical syntheses were performed in a one-compartment cell using a computer-controlled Model 273 potentiostat−galvanostat (EG&G Princeton Applied Research). The synthesis of aligned Pth tubules was described in re 20, and also see Supporting Information.[20] After the growth of Pth nanotubules, the stainless steel was taken away; overturn the membrane to make the gold layer face the counter electrode. A platinum wire with a diameter of 0.2 mm was connected to the gold layer for connecting the working electrode to the potentiostat. The membrane with the platinum wire was fixed between two Teflon rings and used as the working electrode. Then a compact Pth film was grown on the surface of the gold layer under the same electrochemical conditions used for the growth of Pth tubules. Free-standing bilayer film with a Pth tubule layer and a compact Pth layer was obtained by dissolving the AAO template with NaOH. After being washed repeatedly with distilled water, a diluted HCl solution was used to neutralize the bilayer film and washed again with distilled water to ensure the pH of the medium around or slightly lower than 7 to remove the residual OH^- in the film, avoiding the reaction of OH^- species with glass (SiO_2) during the drying process. The surface morphology of the samples was studied by using a scanning electron microscope (FEI Sirion 200, Japan). Raman spectrum was recorded on a RM 2000 microscopic confocal Raman spectrometer (Renishaw, UK) with an excitation of 632.8 nm laser light at 0.5 mW. X-ray photoelectron energy spectroscopic (XPS) examinations were performed by the use of a ESCALAB 220i-XL spectrometer (VG, UK).

Adhesion Force Measurements. To investigate the adhesion force, a Pth bilayer film in the wet state was collected by a clean glass with its aligned nanotubule surface in contact with the glass surface. After the drying of a Pth bilayer film on a target surface, another clean glass slide with a metallic hook on it (for normal force measurements) or only a clean glass slide (for shear force measurement) was glued on the compact surface of the bilayer film as a supporting substrate by 5 min epoxy. The epoxy adhesive was coated on the central region of the bilayer film with an area smaller than that of the polymer film. The compact Pth layer together with the thin gold layer on the backside of the Pth nanotubule layer successively prevented the penetration of epoxy through the Pth bilayer film to pollute the Pth nanotubule surface. To further exclude the possibility of the epoxy adhesive creeping up to the stalks of the specimen, we precured the epoxy gel for about 1 min before applying it to the specimen. Successively, we wiped off the marginal polymer film around the supporting glass by a knife or controlled the area of epoxy coating to make the sample size slightly larger than the area with epoxy adhesive (Figure 5). Then, another hook was glued to the backside of the substrate glass for measuring the normal pull-off force (*i.e.*, normal adhesion force, Figure 5a) or a SS foil (1.5 cm × 5.0 cm × 1.0 mm) was glued on the edge of each glass slide for measuring the parallel pull-off force (*i.e.*, shear adhesion force, Figure 5b). The sample sizes were controlled to be 0.5−1.0 cm^2. Other smooth surfaces, such as freshly cleaved mica, GaAs wafer, highly cleaned poly(methyl methacrylate), and Teflon plates, were also used for collecting the Pth bilayer films.

Recovery of the Used Pth Bilayer Adhesives. (1) Electrochemical route: after detachment from the target surface, the glass supported Pth bilayer film was used as the working electrode; a stainless steel sheet was used as the counter electrode, and a Ag/AgCl wire was used the counter electrode. The distance between the counter and working electrodes was 0.5 cm. Freshly distilled BFEE was used as the electrolyte, and it was deoxygenated by bubbling dry pure N_2 gas. Then, the film was treated by voltammetric scanning in the potential range of −0.5 to 1.0 V at

a scan rate of 0.1 V s^{-1} for five cycles and finally stopped at −0.5 V. Successively, the film was washed extensively with water or ethanol for dry adhesives. (2) Chemical route: the film was immersed in KOH (0.1 mol L^{-1}) for 2 h and then washed extensively with HCl (0.1 mol L^{-1}), and successively with water or 90% ethanol for dry adhesives. The normal adhesion forces of the reused films were measured to be 67 ± 10 N cm^{-2} for method 1 and 55 ± 8 N cm^{-2} for method 2, respectively.

Acknowledgment. This work was supported by the National Natural Science Foundation of China (50533030, 20774056, and 20604013) and 863 Projects (2006AA03Z105). We are grateful to Yugui Jiang and Xi Zhang from Tsinghua University for their assistance in the contact angle and surface energy measurements.

Supporting Information Available: Fabrication of the Pth bilayer film, surface characterizations, characterization of Pth nanotubule surfaces, Young's modulus measurements, choice of stretching rate for adhesion force measurements, adhesion force−time dependence of the Pth bilayer film, contact angle and surface energy measurements. This material is available free of charge *via* the Internet at http://pubs.acs.org.

REFERENCES AND NOTES

1. Autumn, K.; Liang, Y. A.; Hsieh, S. T.; Zesch, W.; Chan, W. P.; Kenny, T. W.; Fearing, R.; Full, R. J. Adhesive Force of a Single Gecko Foot-Hair. *Nature* **2000**, *405*, 681–685.
2. Autumn, K. How Gecko Toes Stick-The Powerful, Fantastic Adhesive Used by Geckos Is Made of Nanoscale Hairs That Engage Tiny Forces, Inspiring Envy Among Human Imitators. *Am. Sci.* **2006**, *94*, 124–132.
3. Ghatak, A.; Mahadevan, L.; Chung, J. Y.; Chaudhury, M. K.; Shenoy, V. Peeling From a Biomimetically Patterned Thin Elastic Film. *Proc. R. Soc. A* **2004**, *460*, 2725–2735.
4. Gorb, S.; Varenberg, M.; Peressadko, A.; Tuma, J. Biomimetic Mushroom-Shaped Fibrillar Adhesive Microstructure. *J. R. Soc. Interface* **2007**, *4*, 271–275.
5. Kim, S.; Sitti, M. Biologically Inspired Polymer Microfibers with Spatulate Tips as Repeatable Fibrillar Adhesives. *Appl. Phys. Lett.* **2006**, *89*, 262911.
6. Majumder, A.; Ghatak, A.; Sharma, A. Microfluidic Adhesion Induced by Subsurface Microstructures. *Science* **2007**, *318*, 258–261.
7. Reddy, S.; Arzt, E.; del Campo, A. Bioinspired Surfaces with Switchable Adhesion. *Adv. Mater.* **2007**, *19*, 3833–3837.
8. Crosby, A. J.; Hageman, M.; Duncan, A. Controlling Polymer Adhesion with "Pancakes". *Langmuir* **2005**, *21*, 11738–11743.
9. del Campo, A.; Arzt, E. Design Parameters and Current Fabrication Approaches for Developing Bioinspired Dry Adhesives. *Macromol. Biosci.* **2007**, *7*, 118–127.
10. Geim, A. K.; Dubonos, S. V.; Grigorieva, I. V.; Novoselov, K. S.; Zhukov, A. A.; Shapoval, S. Y. Microfabricated Adhesive Mimicking Gecko Foot-Hair. *Nat. Mater.* **2003**, *2*, 461–463.
11. Lee, H.; Lee, B. P.; Messersmith, P. B. A Reversible Wet/Dry Adhesive Inspired by Mussels and Geckos. *Nature* **2007**, *448*, 338–341.
12. Mahmood, N.; Busse, K.; Kressler, J. Investigations on the Adhesion and Interfacial Properties of Polyurethane Foam/Thermoplastic Materials. *J. Appl. Polym. Sci.* **2007**, *104*, 479–488.
13. Ge, L.; Sethi, S.; Ci, L.; Ajayan, P. M.; Dhinojwala, A. Carbon Nanotube-Based Synthetic Gecko Tapes. *Proc. Natl. Acad. Sci. U.S.A.* **2007**, *104*, 10792–10795.
14. Qu, L.; Dai, L. Gecko-Foot-Mimetic Aligned Single-Walled Carbon Nanotube Dry Adhesives with Unique Electrical and Thermal Properties. *Adv. Mater.* **2007**, *19*, 3844–3849.
15. Sethi, S.; Ge, L.; Ci, L.; Ajayan, P. M.; Dhinojwala, A. Gecko-Inspired Carbon Nanotube-Based Self-Cleaning Adhesives. *Nano Lett.* **2008**, *8*, 822–825.
16. Yurdumakan, B.; Raravikar, N. R.; Ajayan, P. M.; Dhinojwala, A. Synthetic Gecko Foot-Hairs from Multiwalled Carbon Nanotubes. *Chem. Commun.* **2005**, 3799–3801.
17. Zhao, Y.; Tong, T.; Delzeit, L.; Kashani, A.; Meyyappan, M.; Majumdar, A. Interfacial Energy and Strength of Multiwalled-Carbon-Nanotube-Based Dry Adhesive. *J. Vac. Sci. Technol., B* **2006**, *24*, 331–335.
18. Sitti, M.; Fearing, R. S. Synthetic Gecko Foot-Hair Micro/Nano-Structures as Dry Adhesives. *J. Adhes. Sci. Technol.* **2003**, *17*, 1055–1073.
19. Shi, G. Q.; Jin, S.; Xue, G.; Li, C. A Conducting Polymer Film Stronger than Aluminum. *Science* **1995**, *267*, 994–996.
20. Fu, M. X.; Zhu, Y. F.; Tan, R. Q.; Shi, G. Q. Aligned Polythiophene Micro- and Nanotubules. *Adv. Mater.* **2001**, *13*, 1874–1877.
21. del Campo, A.; Arzt, E. Fabrication Approaches for Generating Complex Micro- and Nanopatterns on Polymeric Surfaces. *Chem. Rev.* **2008**, *108*, 911–945.
22. Autumn, K.; Dittmore, A.; Santos, D.; Spenko, M.; Cutkosky, M. Frictional Adhesion: A New Angle on Gecko Attachment. *J. Exp. Biol.* **2006**, *209*, 3569–3579.
23. Autumn, K.; Sitti, M.; Liang, Y. A.; Peattie, A. M.; Hansen, W. R.; Sponberg, S.; Kenny, T. W.; Fearing, R.; Israelachvili, J. N.; Full, R. J. Evidence for van der Waals Adhesion in Gecko Setae. *Proc. Natl. Acad. Sci. U.S.A.* **2002**, *99*, 12252–12256.
24. Kendall, K. Adhesion—Molecules and Mechanics. *Science* **1994**, *263*, 1720–1725.
25. Aksak, B.; Murphy, M. P.; Sitti, M. Adhesion of Biologically Inspired Vertical and Angled Polymer Microfiber Arrays. *Langmuir* **2007**, *23*, 3322–3332.
26. Autumn, K.; Peattie, A. M. Mechanisms of Adhesion in Geckos. *Integr. Comp. Biol.* **2002**, *42*, 1081–1090.
27. Jiang, Y. G.; Wang, Z. Q.; Xu, H. P.; Chen, H; Zhang, X.; Smet, M.; Dehaen, M.; Hirano, Y.; Ozaki, Y. Investigation into pH-Responsive Self-Assembled Monolayers of Acylated Anthranilate-Terminated Alkanethiol on a Gold Surface. *Langmuir* **2006**, *22*, 3715–3720.
28. Clint, J. H.; Wicks, A. C. Adhesion under Water: Surface Energy Considerations. *Int. J. Adhes. Adhes.* **2001**, *21*, 267–273.
29. Lim, K. B.; Lee, D. C. Surface Modification of Glass and Glass fibres by Plasma Surface Treatment. *Surf. Interface Anal.* **2004**, *36*, 254–258.
30. Maboudian, R.; Howe, R. T. Critical Review: Adhesion in Surface Micromechanical Structures. *J. Vac. Sci. Technol., B* **1997**, *15*, 1–20.
31. Autumn, K.; Gravish, N. Gecko Adhesion: Evolutionary Nanotechnology. *Philos. Trans. R Soc. A* **2008**, *366*, 1575–1590.
32. Fu, M. X.; Shi, G. Q.; Chen, F. G.; Hong, X. Y. Doping Level Change of Polythiophene Film during its Electrochemical Growth Process. *Phys. Chem. Chem. Phys.* **2002**, *4*, 2685–2690.